

Stable soliton *vs* collapse dynamics of short laser pulses in nonlinear structures with intermediate dimensionality *

Dima Cheskis¹, Shimshon Bar-Ad^{1,*}, Roberto Morandotti²,
J. Stewart Aitchison³, Hagai S. Eisenberg^{4,5}, Yaron Silberberg⁵,
and Duncan Ross⁶

¹*School of Physics and Astronomy, Raymond and Beverly Sackler
Faculty of Exact Sciences, Tel Aviv University, Tel Aviv 69978, Israel*

²*INRS-Énergie et Matériaux,
Université du Québec, Varennes, Québec J3X 1S2, Canada*

³*Department of Electrical and Computer Engineering,
University of Toronto, Toronto, Ontario M5S 3G4, Canada*

⁴*Department of Physics,
University of California, Santa Barbara, CA 93106, USA*

⁵*Department of Physics of Complex Systems,
Weizmann Institute of Science, Rehovot 76100, Israel*

⁶*Department of Electronics and Electrical Engineering,
University of Glasgow, Glasgow G12 8QQ, Scotland, UK*

* *Corresponding author: shimshon@post.tau.ac.il*

Received 15 October 2003, accepted 5 March 2004

Abstract

We investigate the propagation of short laser pulses in arrays of coupled nonlinear waveguides. In the experiment we inject intense 60-fs pulses into planar silica waveguide arrays, with the laser tuned to the anomalous dispersion regime. Depending on the excitation conditions, either collapse dynamics is observed, or trapping of the pulse in a single waveguide. The collapse dynamics in these intermediate

*Presented at Russian-Israeli Conference *Frontiers in Condensed Matter Physics*.
Shoresh, Israel, 19-24 October 2003

dimensionality structures are similar to those previously observed in the perfect two-dimensional configuration. On the other hand, an extremely sharp transition is observed, from strong diffraction at low powers to strong localization at high powers, when the pulses are injected into a single waveguide. This behavior suggests the existence of a range of parameters where quasi-stable spatiotemporal solitons may form. Our numerical simulations demonstrate that high-order dispersion is essential for an effective arrest of the collapse in these Kerr media, and lend further support to the interpretation of the experimental data as an indication for quasi-stable propagation.

PACS: 42.65.Tg, 42.65.Sf, 42.65.Jx, 42.65.Wi

Optical solitons are localized electromagnetic waves that propagate in nonlinear media where dispersion and/or diffraction are present. They are the most thoroughly studied form of solitons, in view of their potential application in optical communications and switching devices. One-dimensional optical solitons, that exhibit confinement in one transverse dimension (either spatial or temporal), have been the subject of extensive theoretical and experimental studies [1]. Multidimensional solitons, on the other hand, and spatiotemporal solitons (STS) in particular, have received far less attention. A most intriguing type of STS forms when diffraction and dispersion have the same magnitude. In this situation the nonlinearity may simultaneously balance both, leading to the formation of an STS that is symmetrical in all transverse dimensions. Such STS are sometimes called "light bullets", and were originally proposed in the context of media with a positive Kerr nonlinearity and anomalous dispersion [2]. However, even a simple analysis can show that only one-dimensional Kerr solitons are stable, while multidimensional solitons are not [2]. This instability occurs since the slightest perturbation of the soliton's power or size results in a breakup of the delicate balance between dispersion, diffraction and the nonlinearity. If dispersion and diffraction win, the result is a spread-out of the wave packet. On the other hand, if the nonlinearity becomes dominant, the wave packet experiences a catastrophic self-focusing in all transverse dimensions, known as "collapse". It should be emphasized, though, that such a mathematical collapse to a singularity has not been observed experimentally. It is usually avoided in experiments due to higher-order nonlinearities and dispersion, that become increasingly important during the collapse.

Collapse dynamics in Kerr media were recently demonstrated using a planar glass waveguide, where the pulse disperses in one dimension and diffracts in another [3]. This particular configuration is one example of a

"1+2" case, where the "1" denotes the direction of propagation and the "2" refers to the number of transverse dimensions in which the wave packet can diffract or disperse. In that experiment simultaneous spatial and temporal self-focusing was observed in the anomalous dispersion regime, and multi-photon absorption (MPA) and stimulated Raman scattering (SRS) were suggested as possible mechanisms that arrest the collapse. In parallel, STS have been generated in bulk quadratic media, in which case stable propagation was demonstrated in the temporal dimension and in one spatial dimension, while diffraction occurred in the remaining spatial dimension [4]. Thus, the realization of a true STS, especially in Kerr media, remains an important goal in the field of soliton physics.

A particularly interesting situation arises when a pulse propagates in structures with intermediate dimensionality, such as planar arrays of coupled one-dimensional waveguides. Such periodic arrays are one-dimensional photonic crystals, and in many respects their behavior is intermediate between one-dimensional ("1+1") and two-dimensional ("1+2"). Diffraction in these structures takes the form of a weak coupling between adjacent waveguides, and leads to a characteristic discrete diffraction where the light distribution has the form of a Bessel function [5]. Spatial solitons that form in these arrays are known as discrete solitons. They have been studied extensively both theoretically [6] and experimentally [7], and shown to possess several novel and intriguing dynamical properties. For example, both stable and unstable spatial solitons have been demonstrated, and the difference of energy between the two (called the Peierls-Nabarro potential) accounts for the tendency of discrete solitons to lock to the waveguide direction at high powers, or to acquire transverse momentum and shift laterally, depending on the input parameters [8]. Moreover, the sign and value of diffraction in waveguide arrays is a function of the propagation direction [9], with important consequences to the linear and nonlinear properties [10]. These special properties of structures with intermediate dimensionality, coupled with the known dependence of STS stability on the number of transverse dimensions, provide a strong motivation for the study of STS and collapse dynamics in planar waveguide arrays.

The properties of discrete solitons have been studied extensively in AlGaAs waveguide arrays [7, 8, 10]. However, AlGaAs has a normal dispersion, and therefore cannot support STS. Thus the case of anomalous dispersion, which is a prerequisite for the formation of STS, has been studied only theoretically. These studies have concluded that the differences between discrete and continuum STS are expected to be significant. In particular, it has been suggested that the instability and collapse of STS in the planar geometry

would disappear in coupled waveguide arrays. Using coupled mode theory, in the form of linearly coupled one-dimensional nonlinear Schrödinger equations (NLSE), Aceves et al. have shown that the discrete nature of the structure effectively acts as a saturable nonlinearity, and instead of a catastrophic collapse, energy localization in a single waveguide is expected, accompanied by strong temporal compression [11]. The localization and temporal compression in an array were demonstrated numerically [11]. Self trapping was also demonstrated numerically [12]. However, the necessary initial conditions for such STS-like behavior were not clearly identified.

In this work we present experimental evidence for such strong spatial localization in a single waveguide, when the array is excited in the anomalous dispersion regime. We use arrays of silica glass, where the dispersion is anomalous for laser pulses with wavelengths in the optical communication window ($\lambda \approx 1.5\mu\text{m}$). We employ two different experimental configurations, that result in different initial conditions: a broad input beam and single waveguide excitation. The behavior that we observe with a broad input beam is reminiscent of the collapse dynamics in the "1+2" case [3]. On the other hand, with single waveguide excitation we observe an extremely sharp transition, as a function of the input power, from a regime of strong diffraction to a regime of strong spatial localization. The broad regime of strong spatial localization, in which the beam locks to a single waveguide, suggests that a range of parameters may exist where quasi-stable STS may form. We also present numerical simulations that demonstrate that high-order dispersion is essential for an effective arrest of the collapse, and show that at certain powers a quasi-stable asymmetric pulse indeed forms. This lends further support to the interpretation of the experimental data as an indication for quasi-stable propagation.

The sample that we used is 2.5 cm long, and consists of several one-dimensional periodic arrays, each with 101 weakly-coupled optical waveguides, buried inside a layer of flame hydrolysis deposited silica. The core of each single-mode waveguide is germanium-boron doped silica, has a square cross section of $4\mu\text{m} \times 4\mu\text{m}$, and is surrounded by a silica cladding. The refractive index step between the cladding and the core is $\Delta n = 0.75\%$. The period of the different arrays d (see Fig. 1) varies between $11\mu\text{m}$ and $13\mu\text{m}$, in order to modify the degree of coupling between adjacent waveguides. We inject transform-limited 60 fs pulses, at a wavelength of 1520 nm and with peak powers up to 2MW, generated by a Spectra Physics OPA 800 optical parametric amplifier. The spatial profile of the input beam is varied as to excite just one or several waveguides. A microscope objective and a cylindrical lens are combined in order to obtain an elliptical input beam, $\simeq 170\mu\text{m}$ wide,

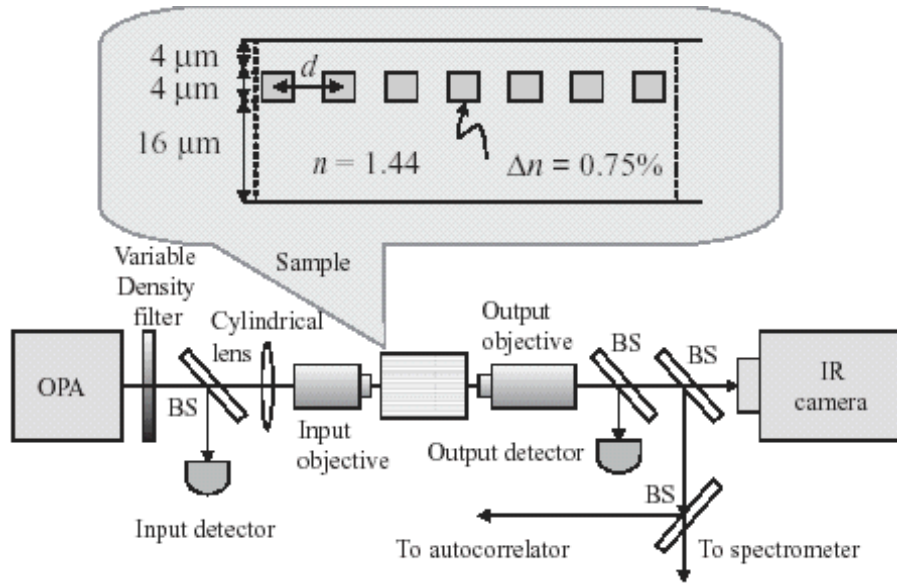


Figure 1: Experimental setup and sample cross-section.

with a flat phase front at the input facet of the sample. This arrangement allows matching of the beam size, and thereby the diffraction length, to the dispersion length. The cylindrical lens may be removed to allow single waveguide excitation. The output facet of the sample is imaged onto an infrared camera. A portion of the beam is directed to a spectrometer, and another portion to a non-collinear autocorrelator. The $100\mu\text{m}$ thick BBO crystal in the autocorrelator allows accurate measurements of pulse durations down to 10 fs, and the glass in the optical path to the autocorrelator introduces a systematic error of less than 10 fs in the measurements. An aperture, placed in an image plane of the output facet, allows temporal and spectral characterization of the central part of the output beam. The spatial cross-section, power spectrum, autocorrelation and output power are measured as functions of the input power. The experimental data shows little variations between the different arrays, and the results presented here are typical to all of them.

Fig. 2 presents images of the sample's output facet, recorded under different excitation conditions. Fig. 2a and Fig. 2b were both obtained with a broad input beam (i.e. equal dispersion and diffraction lengths). The three images in Fig. 2a depict a stable spatial soliton, and correspond to

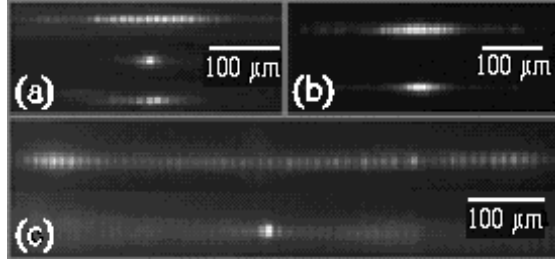


Figure 2: Images of the sample's output facet under different excitation conditions: (a) broad input beam (equal dispersion and diffraction lengths): top to bottom - 0.09MW, 0.45MW, 0.74MW; (b) the unstable mode is excited with the broad input beam: top - low power; bottom - high power; (c) single waveguide excitation: top - 0.07MW; bottom - 0.44MW.

the lowest input power, maximum spatial compression and maximum input power (top to bottom). It can be seen that as the power of the incoming beam is increased, the beam width first contracts to about $10\mu\text{m}$, and then gradually broadens. At the minimum width most of the pulse energy is concentrated in a single waveguide, with two small satellite pulses in the neighboring waveguides. A small tilt of the input facet relative to the input beam allows excitation of an unstable soliton, which is peculiar to the array [8]. As seen in Fig. 2b, the self-focusing obtained in this case is rather weak. In contrast, the spatial compression of the stable soliton is remarkable. It is substantially stronger than that observed in the case of normal dispersion [7] and is also more pronounced than the compression in the perfect planar configuration [3].

Next we focus on the dynamics of the stable spatial mode of the array. Its evolution as function of input power is presented in Fig. 3 in the form of 10 spatial cross sections of the beam at the output facet. The corresponding variations of the beam width and pulse duration are plotted in Fig. 5a, which shows that the strongest spatial compression lags slightly behind the maximum temporal compression. This may be partly due to a small mismatch between the dispersion and diffraction lengths. More importantly, and in contrast with the results obtained under similar conditions in the "1+2" case [3], there is a clear asymmetry in the compression: the output beam decreases by a factor of ≈ 10 relative to its width at the input facet, but the pulse duration decreases only slightly (by less than 10%). This behavior demonstrates that the symmetry between the spatial and temporal

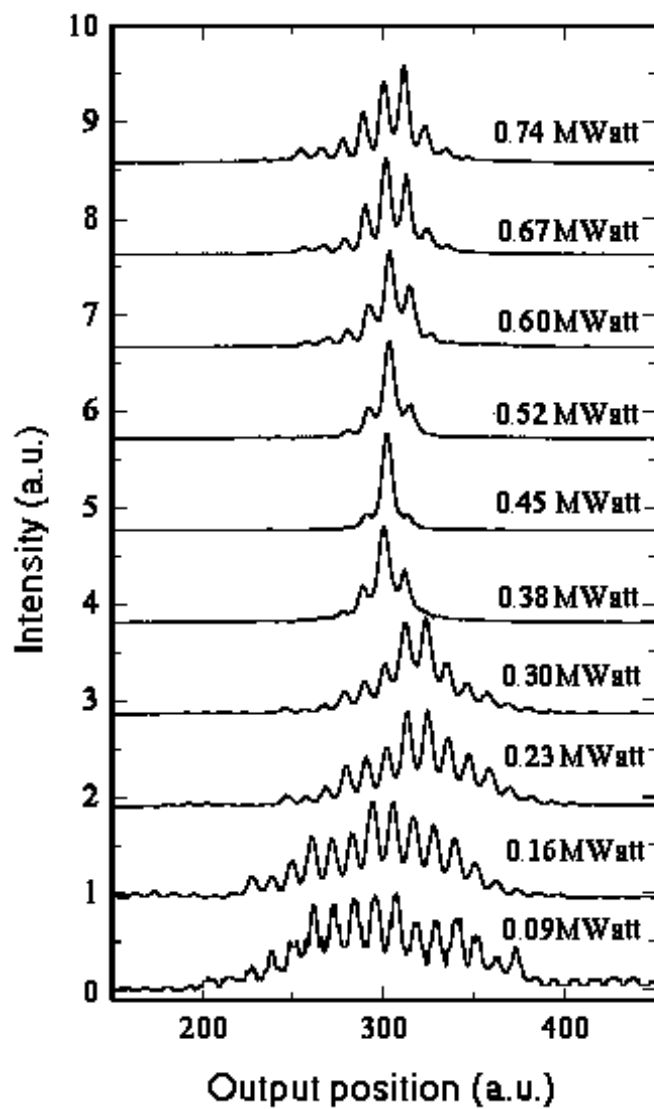


Figure 3: Spatial cross sections at the output facet, measured as function of input peak power, with a broad input beam.

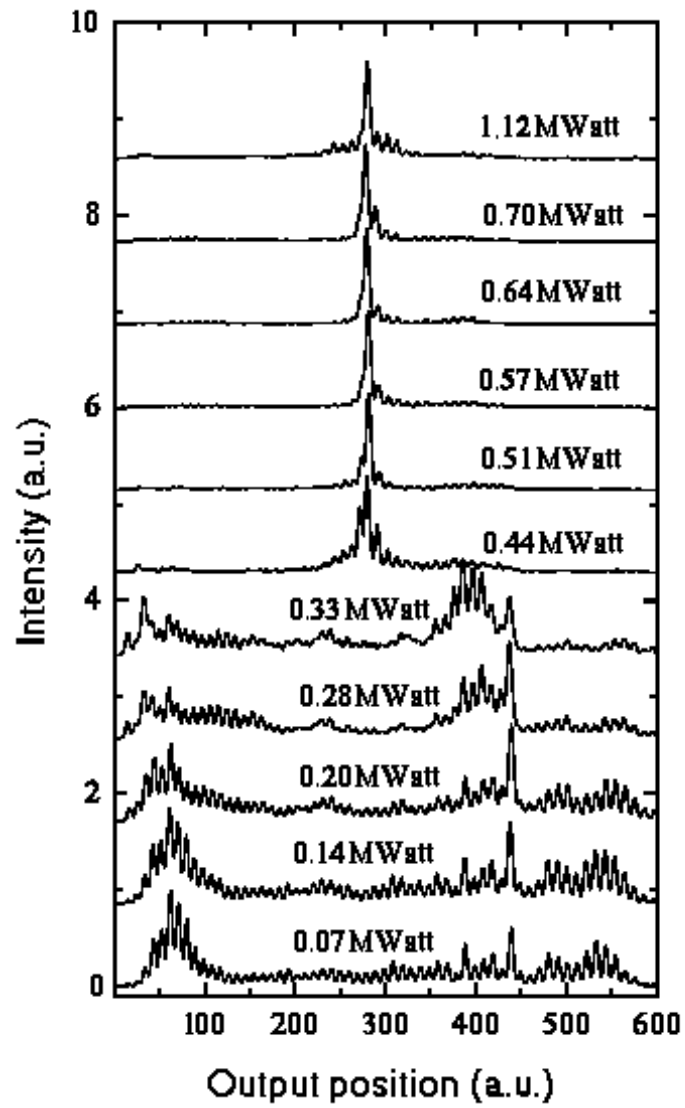


Figure 4: Spatial cross sections at the output facet, measured as function of input peak power, for single waveguide excitation.

coordinates is broken, and strongly suggests that the sudden onset of significant nonlinear effects, as the pulse compresses into a single waveguide, induces temporal broadening followed by diffraction. Thus the symmetry breaking in the array indeed restrains the collapse. Except for the pronounced asymmetry described above, the behavior that we observe with a broad input beam is very similar to the quasi-collapse in two dimensions [3]. Yet, the dynamics at high input powers, beyond the point of maximum compression, reveals more subtle differences between the two geometries. As the spectral data in Fig. 5b demonstrate, the spectrum of the output beam mainly broadens before maximum compression is achieved but beyond that point the spectrum strongly shifts to longer wavelengths. The shift is due to SRS and is accompanied by a significant broadening of the pulse (Fig. 5a). This effectively breaks the symmetry between the spatial and temporal coordinates and stops the compression. The broadened pulse then starts to diffract. The diffraction is more regular than in the two-dimensional case, where a break-up of the beam to filaments was observed at high input power [3]. Also in contrast with the two-dimensional case [3], in the present experiment the output power is proportional to the input power, and there is no evidence for nonlinear loss. This fact suggests that the maximum power density attained within the array is lower, which also shows that the array restrains the collapse more effectively.

A totally different picture is observed when the input beam is focused into a single waveguide. At low input powers the beam strongly diffracts [top image in Fig. 2c], and shows the characteristic Bessel function light distribution of discrete diffraction [5]. Beyond a certain, well-defined input power, however, the beam abruptly contracts, and all the power is essentially localized in one waveguide [bottom image in Fig. 2c]. The spatial distribution at the output facet then shows very little changes as the input power is further increased. The variation of the beam width at the output facet as function of the input power and the corresponding changes of the pulse duration and spectrum are plotted in Figs. 5a and 5c. The evolution of the spatial profile as function of input power is seen in Fig. 4, where 11 spatial cross sections of the beam at the output facet are plotted. Two different regimes are clearly seen, with an extremely sharp transition between them. Also note that the pulse duration at the output facet increases monotonically, and that following the abrupt localization in a single waveguide the temporal broadening and red shift due to SRS increase dramatically. As in the case of broad beam excitation, the output power is proportional to the input power and there is no evidence for nonlinear loss. In particular, this means that the fixed spatial distribution that we observe does not correspond to a well-defined

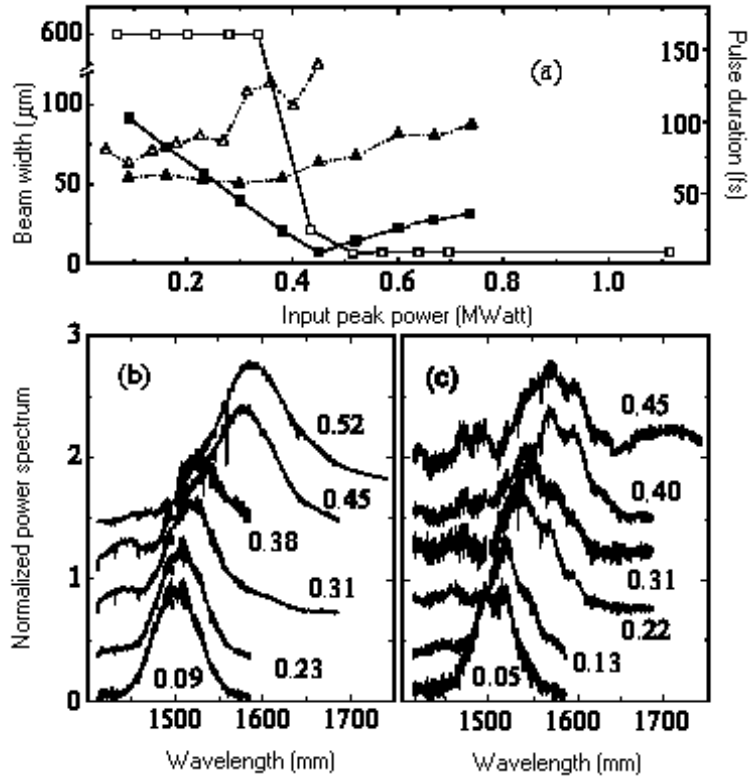


Figure 5: Spatial, temporal and spectral data obtained with different excitation parameters: (a) the variations, as function of input power, of the beam width (squares) and pulse duration (triangles), for a broad input beam (full symbols) and for single waveguide excitation (open symbols); (b) and (c) show the evolution of the output spectrum as function of the input peak power for a broad input beam and for single waveguide excitation, respectively (the spectral curves are displaced vertically for better clarity, and the numbers next to the traces indicate the input peak powers in MW).

pulse energy. Rather, the pulse energy increases as the pulse broadens in the time domain. The peak power at which the trapping occurs is $\approx 0.4 \times 10^6$ W, which is 100 times lower than the peak power of a 60 fs one-dimensional soliton, but consistent with a pulse compressed to 6 fs. Clearly, other effects must intervene to broaden the pulse before it reaches the output facet of the sample. We also note that the observed variation of the output wave packet size as function of its energy is exactly the opposite of that expected of a perfect one-dimensional light bullet in Kerr media [2]. This means that the localization in a single waveguide should not be understood as just a trivial decoupling of the waveguides due to the nonlinearity.

It is clear from the experimental data that higher-order nonlinearities, beyond the Kerr nonlinearity, significantly modify and complicate the dynamics of the propagating pulse. In particular, the temporal compression proposed by Aceves et al. [11] is not observed in our experiment. SRS is an obvious reason for the deviations that we observe from the theoretical predictions, and these may also result from high-order dispersion, which becomes significant as the pulse strongly compresses and as its spectrum broadens and shifts to longer wavelengths. Nevertheless, the broad regime of strong spatial localization that we observe in the case of single waveguide excitation suggests the existence of a range of parameters where quasi-stable propagation may actually occur. Since we are only able to characterize the pulses at the sample's output facet, our experiment does not give a direct and conclusive evidence for such quasi-stable propagation. However, it is very unlikely that the pulse, which is initially localized in a single waveguide, undergoes some unexpected dynamics inside the sample before re-emerging at the output facet in a localized state. More likely, once the nonlinearity is strong enough to overcome the diffraction of the narrow input beam, the pulse is trapped in a single waveguide, and propagates a distance of several centimeters without significantly changing its shape. Such a trapped pulse is definitely not a symmetrical optical bullet [2], but it is stable in the sense that its shape does not vary dramatically as the input power is further increased. In particular, as the input power is increased, self focusing does not completely overcome the other processes that tend to broaden the wave packet, and the collapse is arrested. On the other hand, it is obvious that the strong SRS at very high input powers must result from a strong temporal contraction of the pulse, and since this contraction is not observed in the experiment, it is most likely that at these input powers the pulse initially contracts, and then broadens again, as a result of high-order dispersion.

To demonstrate these effects we have compared our experimental results to two-dimensional numerical simulations of the NLSE [3] that use the split-

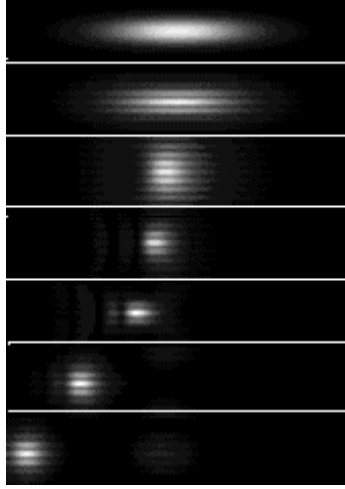


Figure 6: Data from a numerical simulation, showing the evolution of the spatiotemporal profile of the pulse as it propagates through the sample. Each frame is a spatiotemporal contour plot of the pulse at a given distance from the input facet, and the horizontal and vertical coordinates are time and space, respectively. The size of each window is 119fs by $114\mu\text{m}$. The distances from the input facet are (from top to bottom): 2.92, 5.83, 17.5, 26.25, 35, 49.6 and 64.17mm. The parameters of the simulation are discussed in the text (note: the window used in the calculations is 4 times larger than that displayed here, in both transverse directions).

step beam propagation method and take into account SRS, MPA, high-order dispersion (third and fourth orders) and the periodic variation of the refractive index in the array. We find that high-order dispersion is indeed essential for an effective arrest of the collapse. It also induces temporal broadening, limits the spectral broadening and quenches MPA, all in agreement with the experiment. The simulations also show that at intermediate input powers the high-order dispersion results in the formation of an asymmetric pulse, which propagates a finite distance with very slow changes of its envelope. The shape of this trapped pulse depends on the magnitude and sign of the high-order dispersion terms.

Fig. 6 shows a typical result of the simulation, obtained with a 60 fs Gaussian pulse, an input peak power of 3.1×10^5 W, an input beam width of $25\mu\text{m}$, and a sample with a period d of $13\mu\text{m}$. The third-order dispersion coefficient in this simulation is $\beta_3 = 0.3 \text{ ps}^3/\text{Km}$ (about twice the value

obtained from the literature [13] and from the Sellmeier equation), and the fourth-order dispersion coefficient is $\beta_4 = -4.4 \times 10^{-4} \text{ps}^4/\text{Km}$ (the value obtained from the Sellmeier equation). Other parameters of silica glass, such as the group velocity, group velocity dispersion, nonlinear refractive index and Raman coefficients are taken from the literature [13]. Weak MPA is assumed, in the form of a six-photon absorption coefficient of $2 \times 10^{-65} \text{Watt}^{-5} \text{cm}^9$ [14]. Fig. 6 shows the evolution of the spatiotemporal profile of the pulse, each frame being a spatiotemporal contour plot of the pulse at a given distance from the input facet (the horizontal and vertical coordinates are time and space, respectively). The figure demonstrates how the Gaussian input wave packet (frame 1) couples into the waveguides (frame 2), and then starts diffracting, while compressing in the time domain (frame 3). This occurs due to the asymmetry of the input pulse, and an input power that results in the nonlinear length being shorter than the dispersion length but longer than the diffraction length. Eventually the strong temporal focusing increases the power density enough to induce spatial focusing (frame 4), and after propagating 3.5 cm through the sample the pulse is localized essentially in a single waveguide (frame 5). At this point high-order dispersion comes into play, arresting the collapse, and the compressed pulse starts diffracting and dispersing very slowly - note how little it changes as it propagates the last 1.5 cm (frames 6 and 7). The slow shift of the pulse relative to the center of the frame, which moves at the average group velocity, is due to third-order dispersion. High-order dispersion also leads to the eventual spread-out of the wave packet, after propagating a distance of ≈ 8 cm through the sample (not shown). A strong spectral broadening, due to self-phase modulation and SRS, accompanies the above dynamics. Fig. 7 shows the spectra at the input, at the point of maximum compression (3.5 cm behind the input facet, corresponding to frame 5 of Fig. 6) and 7 cm behind the input facet. The strong broadening and red shift of the spectrum are evident, and explain the effectiveness of the high-order dispersion in arresting the collapse.

The results of the numerical simulation presented here are in good agreement with the experimental data. In particular, the quasi-stable propagation after the pulse is trapped supports the interpretation of the experimental data as an indication for bullet-like propagation. The main discrepancy is the fact that the temporal compression is not observed in the experiment. This, however, may be due to technical limitations of our autocorrelator. Another conclusion from our simulations is that the eventual spread-out of the wave packet occurs earlier without fourth-order dispersion. This conclusion is in agreement with a recent theoretical analysis [15], which predicts that a small and negative fourth-order dispersion arrests the collapse and

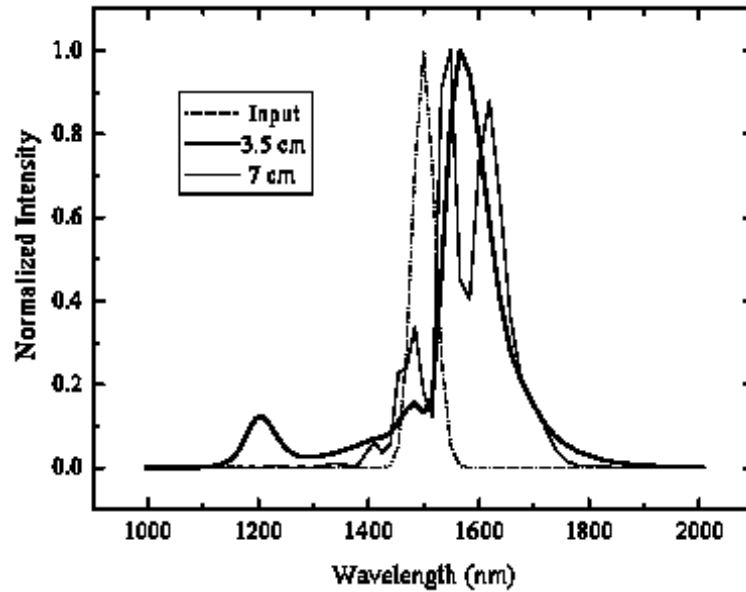


Figure 7: Calculated spectra at different distances from the input facet.

stabilizes optical bullets in Kerr media with dimensionality $d \leq 2$ (in the absence of SRS), and thus lends further support to our interpretation of the experimental data.

This paper is dedicated to the memory of George Thornton of Glasgow University. The research was supported by the Israel Science Foundation and by NSERC in Canada. Valuable discussions with G. Fibich and B. Malomed are acknowledged.

References

- [1] Special issue of J. Opt. Soc. Am. B **14**, 2950 (1997); special issue of Opt. Quantum Electron. B **30**, 501 (1998).
- [2] Y. Silberberg, Opt. Lett. **15**, 1282 (1990).
- [3] H.S. Eisenberg, R. Morandotti, Y. Silberberg, S. Bar-Ad, D. Ross, and J.S. Aitchison, Phys. Rev. Lett. **87**, 043902 (2001).

- [4] X. Liu, L.J. Qian, and F.W. Wise, Phys. Rev. Lett. **82** 4631 (1999); X. Liu, K. Beckwitt, and F. Wise, Phys. Rev. E **62**, 1328 (2000).
- [5] A. Yariv, In: *Optical Electronics*, p. 519 (Saunders College Publishing, Philadelphia, 4th ed., 1991).
- [6] D.N. Christodoulides and R.I. Joseph, Opt. Lett. **13**, 794 (1988).
- [7] H.S. Eisenberg, Y. Silberberg, R. Morandotti, A.R. Boyd, and J.S. Aitchison, Phys. Rev. Lett. **81**, 3383 (1998).
- [8] R. Morandotti, U. Peschel, J.S. Aitchison, H.S. Eisenberg, and Y. Silberberg, Phys. Rev. Lett. **83**, 2726 (1999).
- [9] H.S. Eisenberg, Y. Silberberg, R. Morandotti, and J.S. Aitchison, Phys. Rev. Lett. **85**, 1863 (2000).
- [10] R. Morandotti, H.S. Eisenberg, Y. Silberberg, M. Sorel, and J.S. Aitchison, Phys. Rev. Lett. **86**, 3296 (2001).
- [11] A.B. Aceves, G.G. Luther, C. De Angelis, A.M. Rubenchik, and S.K. Turitsyn, Phys. Rev. Lett. **75**, 73 (1995).
- [12] A.B. Aceves, C. De Angelis, A.M. Rubenchik, and S.K. Turitsyn, Opt. Lett. **19**, 329 (1994).
- [13] G.P. Agrawal, *Nonlinear Fiber Optics* (Academic Press, New York, 1995).
- [14] Six-photon absorption is the lowest-order nonlinear extinction mechanism for $1.5\mu\text{m}$ photons in silica glass; The value chosen for the simulation presented here is approximately 100 times lower than that needed to produce significant extinction for power densities that correspond to trapping of the pulse inside a single waveguide.
- [15] G. Fibich and B. Ilan, Preprint.